Soft Matter

Accepted Manuscript

ROYAL SOCIETY OF CHEMISTRY

www.rsc.org/softmatter

Cite this: DOI: 10.1039/c0xx00000x

www.rsc.org/xxxxxx

ARTICLE TYPE

Insights into the Denaturation of Bovine Serum Albumin with a Thermo-responsive Ionic Liquid

Wenlong Li, and Peiyi Wu*

Received (in XXX, XXX) Xth XXXXXXXXX 20XX, Accepted Xth XXXXXXXXX 20XX

DOI: 10.1039/b000000x

Influence of Bovine Serum Albumin on the phase transition behavior of the synthetic ionic liquid, tetrabutylphosphonium styrenesulfonate ([$P_{4,4,4,4}$][SS]) together with the interactions between [$P_{4,4,4,4}$][SS] and bovine serum Albumin (BSA) were investigated by differential scanning calorimetric (DSC), turbidity measurements, FT-IR, in combination with perturbation correlation moving window (PCMW) and two-dimensional correlation spectroscopy (2Dcos). Our results reveal that the addition of BSA would increase the phase transition temperature but weaken the transition behavior of [$P_{4,4,4,4}$][SS] solution. DSC and turbidity data tell us the transition temperature of ternary system added with 20 wt% BSA is 3 °C higher than 20 %(w/v) [$P_{4,4,4,4}$][SS] solution. Interactions between [$P_{4,4,4,4}$][SS] and BSA together with the phase transition behavior of [$P_{4,4,4,4}$][SS] are responsible for the denaturation of BSA upon heating. PCMW determined the obvious distinctions in LCST of different chemical groups manifesting their various response sequences in the phase separation and denaturation upon heating. Finally, 2Dcos was employed to elucidate the sequence order of chemical group motions during heating. It's worth noting that the appearance of isosbestic point in the C=O groups of FTIR spectra indicates the direct transformation of conformation of α-helix, random coil to β-sheet and β-turn without intermediate transition state. Additionally, the phase separation process of ionic liquid is able to recover to the original status before heating while the denaturation of BSA is irreversible after a cooling process.

Introduction

Since their initial discovery in 1914, ionic liquids (ILs) have been widely investigated in multiple chemistry areas.[1] ILs are collectively known as organic salts whose melting points at or below 100 °C presenting plenty of unique properties,[2, 3] such as good chemical and electro-chemical stability, negligible vapor pressure, low flammability, high ionic conductivity and *etc.*. In most cases, ILs are composed of an organic cation and an organic or inorganic anion. A huge number of potential cation/anion families and their various substitution patterns allow the desired properties for specific applications to be designed. It has been estimated that there can be up to 10^{18} possible combinations of ILs.[4] Because of their excellent properties, ILs have been extensively investigated in various reactions including synthesis,[5, 6] catalysis,[7, 8] analytical chemistry,[1, 9] electrochemistry,[10, 11] and polymerization.[12, 13]

Apart from the above-mentioned applications, ILs which are used to dissolve biomacromolecules such as proteins, celluloses, in "green" chemistry have enjoyed much success and contributed to the rapid evolution of the ionic liquid science.[14, 15] Proteins are usually natural polymeric compounds composed of amino acids linked by peptide bonds. As the constitutional units of many complex biological tissues, proteins are directly relevant to realization of physiological functions. As a result, investigations on proteins have always been the focus and key points of biochemistry and biophysics. As far as studies on proteins and ILs, works by Laszlo[16] and Baker[17] have shown that some proteins are, in fact, soluble and stable in many ILs. Combinations of proteins with ILs have been proposed for various applications, such as protein stabilization,[18] extraction,[19, 20] purification,[21] detection,[22] and crystallization.[23, 24] Besides, it's known that denaturation and aggregation of protein often hampers the efficiency of many biotechnological processes, [8, 18] and limits the lifetime of protein products in the pharmaceutical field.[25] Therefore, understanding the behavior of denaturation and aggregation is crucial for optimizing the production of proteins in many applications. With respect to this, there have been reports about the influence of ILs on the denaturation or aggregation of proteins which is worth mentioning here. Weingärtner characterized the effect of ILs on the thermal denaturation of ribonuclease A (RNase A) near 60 °C and discussed the Hofmeister series of ILs which provided a valuable guide for the understanding in influences of ILs on proteins.[26, 27] Furthermore, the interactions between proteins and ILs were investigated by Figueiredo, who discussed the denaturing/stabilising effects of ILs on proteins.[28]

Recently, thermosensitive or phase transition ionic liquids especially ILs with a lower critical solution temperature (LCST) have led to an eye-catching increase in interests in the relative researches. As one important member of IL family, thermo-

responsive IL, are exhibiting unique advantages in many smart materials.[29, 30] Many studies have referred to the phase separation of ILs,[31, 32] or even PILs[33] in recent years. In 2007, Ohno et al. found a kind of ILs to show unique phase change behavior after mixing them with water.[34] Very recently, Yuan et al. first reported the thermo-responsive IL(TVBP-CxS) and its polymer, cationic PIL with LCST behavior in water.[35] Several ILs including ([$P_{4,4,4,4}$][SS], [$P_{4,4,4,6}$][C3S], [$P_{4,4,4,8}$][C3S], [$P_{4,4,4,8}$][Br], [$N_{4,4,4,4}$][TMBS], [$P_{4,4,4,VB}$][C3S], and [$P_{4,4,4,VB}$][AC3S]) were also confirmed by Ohno to show LCST-type phase separation in aqueous solutions upon heating.[36, 37] As a contrast, the reports on the thermo-responsive ILs and proteins have remained very rare. In consideration of the unique characteristics of proteins and ILs and plenty of existing studies on them, it's believed that combinations of proteins with LCST-type ILs can not only broaden the applications of both proteins and ILs, but also be proposed for more different areas. Under this circumstance, the design of systems including proteins and LCST-type ILs becomes very essential. What's more, comprehension of the mutual interactions between proteins and LCST-type ILs turn out to be of great importance due to its significant help to realize different applications.

Consequently, here we synthesized a LCST-type IL, [$P_{4,4,4,4}$][SS], and designed a ternary composite system composed of [$P_{4,4,4,4}$][SS], BSA and D_2O to explore both the influence of BSA on LCST behavior of IL and the interactions between IL and BSA. To the best of our knowledge, vibrational spectroscopy has been proved to be a quite useful method to trace the changes of individual chemical groups, especially for the thermo-responsive behavior.[38, 39] This is also the first work to employ 2DIR to investigate the molecular microdynamics of protein mixed with thermo-responsive IL. Results revealed that BSA would weaken the phase transition behavior of [$P_{4,4,4,4}$][SS] and increase the LCST of [$P_{4,4,4,4}$][SS] solution. In the meanwhile, interactions between [$P_{4,4,4,4}$][SS] and BSA in combination with the phase transition behavior can induce the denaturation of BSA upon heating. What's worth noting is that the phase separation process is recoverable while the denaturation of BSA is unable to return to the original state after a cooling process. Therefore, through DSC, turbidity measurement, FT-IR, PCMW and 2Dcos analysis, the exact microdynamic mechanism of the phase transition and denaturation process was elucidated. It's helpful for our further comprehensive understanding of the interactions between thermo-sensitive ILs and proteins, which may be useful to facilitate the design of ILs and proteins for thermo-responsive functional materials and biological applications.

Experimental

Materials

Tetrabutylphosphonium bromide ([$P_{4,4,4,4}$]Br), Sodium 4-vinylbenzenesulfonate (Na[SS]) and Albumin from bovine serum (BSA) were purchased from Aladdin. D_2O was purchased from Cambridge Isotope Laboratories Inc. (D-99.9%).

Sample Preparation

The IL, [$P_{4,4,4,4}$][SS], was synthesized by anion exchange reaction of Na[SS] with [$P_{4,4,4,4}$]Br in deionized water for 24 h according to the previous report.[40] The synthetic route of [$P_{4,4,4,4}$][SS] is

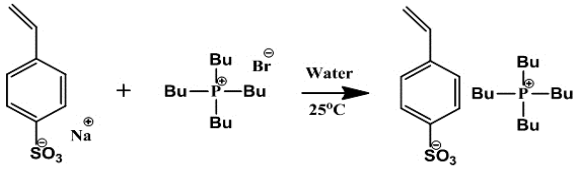

Scheme 1. Synthetic route of [$P_{4,4,4,4}$][SS] thorough anion exchange reaction.

presented in Scheme 1. [$P_{4,4,4,4}$][SS] solution with a concentration of 20 %(w/v) was prepared. And then, BSA (molecular weight, 68000) was added into the solution gradually without any purification. Additionally, the concentration of BSA was calculated with respect to the IL content. To ensure complete dissolution, samples of BSA-[$P_{4,4,4,4}$][SS] solutions were placed at 4 °C for two days before measurements.

Differential Scanning Calorimetry

[$P_{4,4,4,4}$][SS] solutions with concentration of 20 %(w/v) were prepared followed by the addition of BSA into the solutions. The concentrations of BSA in samples for Calorimetric measurements were fixed to 10, 20, 40, 80 wt% respectively. The measurements were performed on a Mettler-Toledo differential scanning calorimeter (DSC) thermal analyzer with a scanning rate of 10 °C/min ranging from 20 to 70 °C.

Turbidity measurements

Turbidity measurements were carried out at 600 nm on a Lamda 35 UV-vis spectrometer at the rate of ca. 0.5 °C/min. The deionized water was used as a reference (100 % transmittance). Temperatures were regulated manually with a water-jacketed cell holder with an interval of 1.0 °C. To control the temperature accurately, each temperature point was held for 2 min. The samples prepared for turbidity measurements were 20 %(w/v) [$P_{4,4,4,4}$][SS] solution and that solution with 20 wt% BSA added.

Fourier Transform Infrared Spectroscopy

The sample of 20 %(w/v) [$P_{4,4,4,4}$][SS]-D_2O solution with 20 wt% BSA for FTIR measurement were prepared by being sealed between two ZnS tablets to prepare a transmission cell. All temperature-resolved FT-IR spectra with a resolution of 4 cm^{-1} were collected on a Nicolet Nexus 6700 spectrometer equipped with a DTGS detector. An electronic cell holder was used to control the rate of temperature increase at ca. 0.5 °C/min. 32 scans were chosen for an all-right signal-to-noise ratio. Temperature-dependent spectra were recorded from 25 to 50 °C at an interval of 1.0 °C during the heating and cooling cycle. After all spectra were collected, the original spectra were baseline-corrected by the software Omnic, ver. 6.1a.[41]

Perturbation correlation moving window (PCMW)

FTIR spectra recorded with an interval of 1°C during the heating-cooling process were used to perform PCMW analysis. Raw data processing was carried out with the method provided by Morita and further calculated by the software 2D Shige, ver. 1.3 (©Shigeaki Morita, Kwansei-Gakuin University, Japan, 2004–2005).[42] An appropriate window size (2m + 1 = 9) was selected to generate PCMW spectra with good quality. At last, the final contour maps were drawn by Origin, ver. 8.0, with red colors

defined as positive intensities while green colors as negative ones.[42]

2D correlation spectroscopy (2DCOS)

FTIR spectra recorded during the heating and cooling processes were also used to perform 2D correlation analysis. The 2D correlation calculation was carried out using the same software, 2D Shige ver. 1.3 (©Shigeaki Morita, Kwansei-Gakuin University, Japan, 2004–2005).[43] Certain wavenumber ranges (3010-2840 and 1700-1600 cm^{-1}) were selected to process the raw data. The contour maps were drawn with red colors representing positive intensities, while green colors representing negative ones by Origin program ver. 8.0.[42]

Results and discussion

Calorimetric measurements

To illuminate the influence of BSA on the phase transition behavior of $[P_{4,4,4,4}][SS]$ solution, differential scanning calorimeter measurements were carried out. DSC heating curves of solutions with BSA at different concentrations are presented in Fig. 1. Obviously, neat IL solution has the biggest endothermic peak and the highest transition temperature during the heating process from 20 to 70 °C. As illustrated in Fig. 1, 20 %(w/v) $[P_{4,4,4,4}][SS]$ solution without BSA shows a phase transition temperature at 36 °C during the heating process. When combined with BSA, the transition temperature of the mixed solutions decrease with the concentration of BSA increasing from 0 to 40 wt%. In the meantime, the endothermic peak of solutions also tend to decrease and become narrow with the rising concentration of BSA indicating that the more BSA added into solution, the weaker enthalpy changes occurring in the phase transition. Closer observation tells us that the transition behavior of $[P_{4,4,4,4}][SS]$ solution with 40 wt% BSA added turns to be very weak. When the concentration of BSA increases to 80 wt%, it's hardly detectable to follow the enthalpy change of the mixed solution during the heating process. In other words, the addition of BSA would hinder and weaken the phase transition behavior of $[P_{4,4,4,4}][SS]$ solution. For further analysis, this may be a result of the new interactions forming between $[P_{4,4,4,4}][SS]$, BSA and

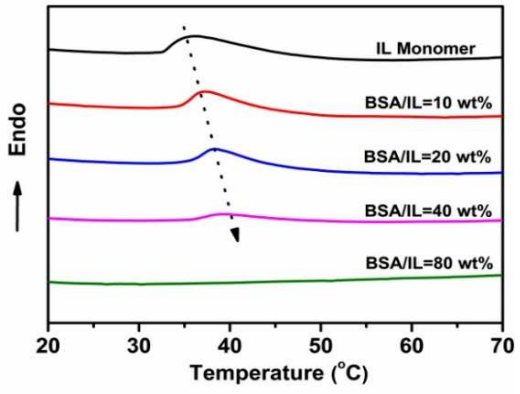

Fig. 1 DSC heating curves of 20 %(w/v) $[P_{4,4,4,4}][SS]$ solutions with addition of BSA whose concentrations are equivalent to 0, 10, 20, 40, 80 wt% of $[P_{4,4,4,4}][SS]$ at the scanning rate of 10 °C/min.

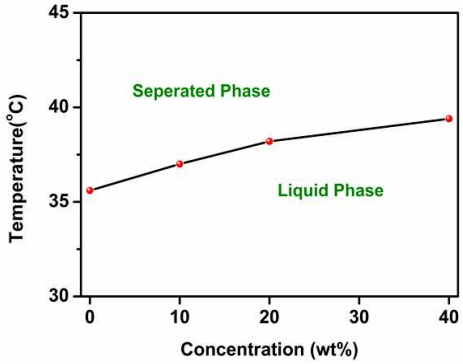

Fig. 2 Phase diagram of Temperature vs. concentration for $[P_{4,4,4,4}][SS]$-BSA-D_2O solution according to the DSC results.

water. These new interactions may reduce the amounts of water interacting with IL which hold the primary responsibility to the phase separation upon heating. Actually, the occurrence of this phenomenon can be attributed to the "Hofmeister effect" investigated by many researchers. On the basis of previous reports, it's known to us that the combination of salts with polymer or protein would influence the behavior of salts and protein or polymer through their interaction with water.[44] This conclusion also suits the behavior of BSA and $[P_{4,4,4,4}][SS]$ well in our work. Maeda reported that ions added into the PNIPAM solution may interact with water and induce changes in the interaction between polymer and water. The indirect effect of the ions might alter the transition temperatures of polymer solutions.[45] It's just the IL rather than polymer behaves in phase separation behavior and BSA can be taken as the Hofmeister salts.

What's worth mentioning is that there must be new interactions between $[P_{4,4,4,4}][SS]$ and BSA, hydrogen bonds and hydrophilic interactions which may contribute to the varying behavior of $[P_{4,4,4,4}][SS]$ upon heating with the increasing BSA concentration in solution. The analysis of these new interactions would be further discussed in the following texts. Additionally, to further illustrate the LCST variation of the $[P_{4,4,4,4}][SS]$-BSA solution, the phase diagram has also been presented in Fig. 2 according to the DSC results.

Turbidity measurements

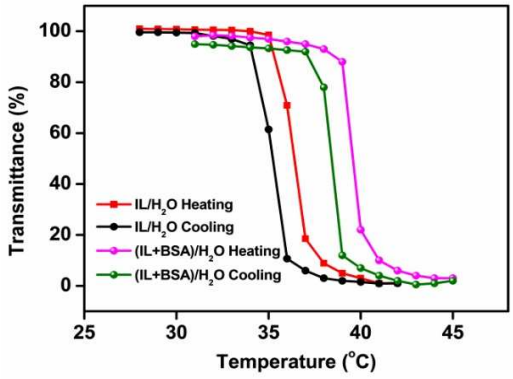

Fig. 3 Turbidity curves of 20 %(w/v) $[P_{4,4,4,4}][SS]$ solution and that solution with the presence of BSA(BSA/IL=20 wt%) during the heating-cooling cycle.

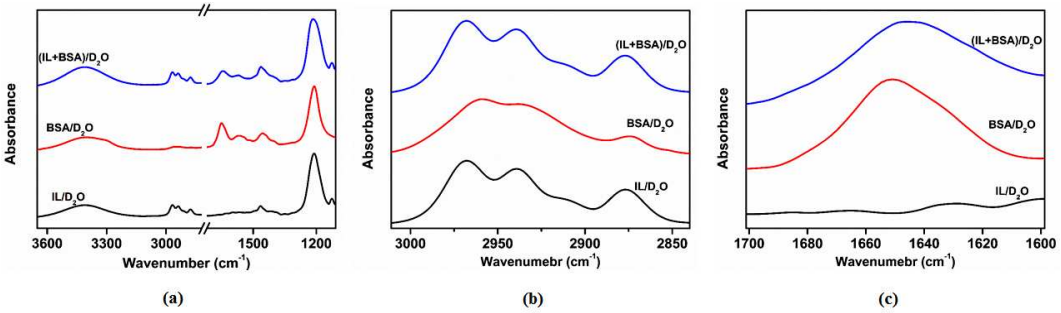

Fig. 4 FT-IR spectra of $[P_{4,4,4,4}][SS]$-D_2O, BSA-D_2O and $[P_{4,4,4,4}][SS]$-BSA-D_2O solutions at room temperature. (a) Full spectra (b) Spectra of C-H region, (c) Spectra of C=O region.

The phase transition behavior of $[P_{4,4,4,4}][SS]$ aqueous solution with BSA is also investigated by turbidity measurements. For comparison and determination of cloud points, 20 %(w/v) $[P_{4,4,4,4}][SS]$ solution and that with the addition of 20 wt% BSA were chosen for experiments. The solutions were measured at an interval of 1.0 °C, as shown in Fig. 3. When it's heated above the transition temperature, the thermo-responsive solutes, $[P_{4,4,4,4}][SS]$, would aggregate together under the driving force of hydrophobic interaction resulting in the rapid drop of transmittance. The cloud point (C_p) is defined as the initial temperature point when transmittance drops below 80 % according to some previous reports.[46, 47]

Obviously seeing in Fig. 3, the cloud point of 20 %(w/v) $[P_{4,4,4,4}][SS]$ solution is about 36 °C while it experiences an increase of 3 °C after added with BSA in the heating process. This indicates the difference in of IL solution with and without BSA which is in accordance with the DSC results. It confirms the increase of transition temperature of $[P_{4,4,4,4}][SS]$ solution with the addition of BSA suggesting that BSA may change the environments and phase transition behavior of IL through new interactions in solution. Additionally, a 1 °C reduction happens to the C_p of both the $[P_{4,4,4,4}][SS]$ solution and that solution with the presence of BSA meaning the existence of slight hysteresis during the cooling process. Now that we have investigated the phase transition phenomena of $[P_{4,4,4,4}][SS]$ solution with addition of BSA upon heating from perspective of thermotics, to further trace the variation of different chemical groups during phase separation from thermodynamic aspect, FTIR measurements are needed.

FTIR analysis

Conventional IR analysis

In FT-IR analysis, D_2O, rather than H_2O, was selected as the solvent to eliminate the overlap of the δ(O-H) band relating to water molecules at about 1630 cm^{-1} with the ν(C=O) of BSA. To plot the characteristic peaks of chemical groups in IL and BSA, FT-IR spectra of 20 %(w/v) $[P_{4,4,4,4}][SS]$-D_2O solution, 20 wt% BSA-D_2O solution and 20 %(w/v) $[P_{4,4,4,4}][SS]$-D_2O solution added with 20 wt% BSA were collected at room temperature, as presented in Fig. 4. Here, two spectral regions are focused on, the C–H stretching band (3010–2840 cm^{-1}), and the amide I (C=O) (1700–1600 cm^{-1}).

It's obvious in Fig. 4(a) that the absorbance of 20 wt% BSA-D_2O solution at 3010-2840 cm^{-1} is a little weak while the absorption of this region for the 20 %(w/v) $[P_{4,4,4,4}][SS]$-D_2O solution is very strong. For closer observation, spectra from 3010 to 2840 cm^{-1} were amplified in Fig. 4(b). From that enlarged spectra, we can find that the absorption of the solution added with BSA is very close to that of 20 %(w/v) $[P_{4,4,4,4}][SS]$-D_2O solution and the C-H peaks of BSA are almost consistent with those of $[P_{4,4,4,4}][SS]$. As a result, this region can be used to discuss the thermodynamic behavior of IL. In the meantime, for the other region, $[P_{4,4,4,4}][SS]$ almost has no absorbance at 1700-1600 cm^{-1} demonstrating that the absorption of solution with the presence of BSA at 1700-1600 cm^{-1} is mainly from C=O groups of BSA, which makes it very convenient to follow the variation of BSA during the phase transition process. For more detailed information in this region, Fig. 4(c) was presented. As a consequence, the absorption of C-H and C=O bands have brought great convenience for the variation of IL and BSA upon heating in this system.

To further expound the phenomenon observed in DSC and turbidity measurements, temperature-dependent FT-IR spectra of 20 % (w/v) $[P_{4,4,4,4}][SS]$-D_2O solution and 20 %(w/v) $[P_{4,4,4,4}][SS]$-20 wt% BSA-D_2O ranging from 25 to 50 °C were carried out respectively, as shown in Fig. 5. Two spectral regions were studied, the C-H stretching band (3010-2840 cm^{-1}), and the C=O bonds (1700-1600 cm^{-1}).

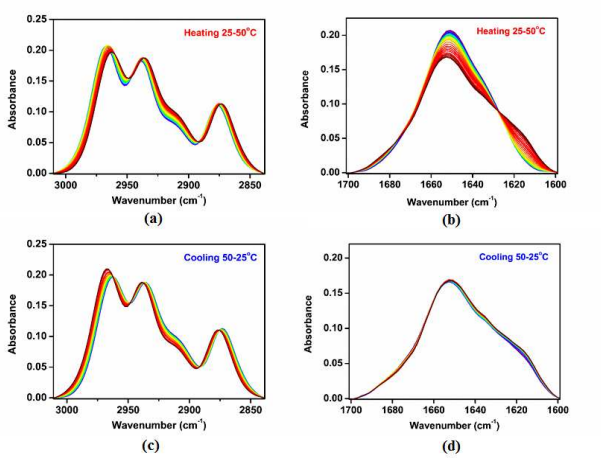

Fig. 5 Temperature-dependent FT-IR spectra of $[P_{4,4,4,4}][SS]$-BSA-D_2O solution ($[P_{4,4,4,4}][SS]/D_2O$ = 20 % (w/v), BSA/$[P_{4,4,4,4}][SS]$ = 20 wt%) in regions of (a) 3010-2840 cm^{-1}, (b) 1700-1600 cm^{-1} during heating and (c) 3010-2840 cm^{-1}, (d) 1700-1600 cm^{-1} during cooling between 25 and 50 °C.

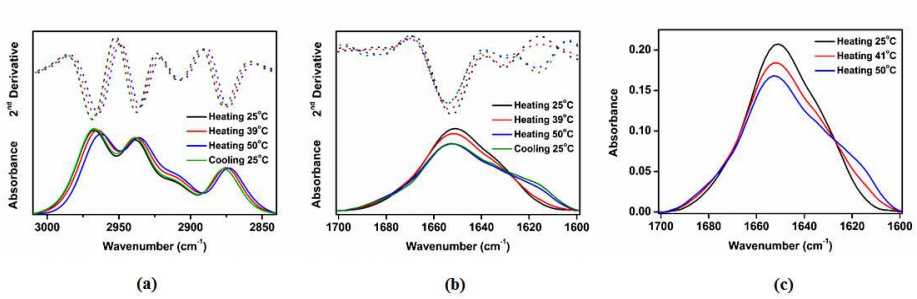

Fig. 6 FTIR and corresponding second-derivate spectra of (a) ν(C-H), (b) ν(C=O) regions of $[P_{4,4,4,4}][SS]$-BSA-D_2O solution at temperatures of 25, 39 and 50 ^oC. (c) FTIR illustration of the isosbestic point for C=O groups at 25, 41 and 50 ^oC.

In Fig. 5, both the C-H and C=O stretching bands show obvious changes upon heating, implying the variation of hydrated interaction and hydrogen bonds in this system. Before the solution was heated, many C-H groups would be hydrated with water molecules presenting relatively high wavenumbers. When the solution was heated, the hydrated interaction and hydrogen bonds between IL, BSA and water would be disrupted. The C-H groups would be transformed into dehydrated status leading to the frequencies of C-H groups shifting to lower wavenumbers, as illustrated in Fig. 5(a). As far as the C=O groups are concerned, they also experience the disruption of hydration and hydrogen bonds with water resulting in the deduction of their integral peak area. It's worth noting that during the heating process, almost all of the C=O region spectra intersect in one point making it an unusual phenomenon.

Observation on the variation of spectra during the cooling process tells us some new information about the changes of chemical groups. It's obvious that the variation of C-H region during cooling is very similar with that in the heating process, as depicted in Fig. 5(a) and 5(c). This demonstrates that the cooling process is basically the recovery of heating process indicating that the variation of C-H groups is mainly phase transition behavior which is revertible. However, there appears rather different phenomenon in Fig. 5(d) comparing with 5(b) that the absorption of C=O groups undergoes great changes upon heating in Fig. 5(b) while the C=O groups almost remain unchanged during the cooling process in Fig. 5(d). Considering this region belongs to the C=O groups of BSA, we deduce that BSA experience a denaturation variation upon heating. After this variation is done, the C=O groups cannot recover to the original state before denaturation.

To enhance the spectral resolution for variation induced by phase separation, FT-IR and second derivative spectra of the two regions at 25, 39 and 50 ^oC are illustrated in Fig. 6. The frequencies of C-H groups would shift to low wavenumbers upon heating demonstrating the dehydration process of C-H groups with water. That is, the water molecules would be stripped out of these interactions transforming C-H into dehydrated status upon heating. The similar phenomenon which can also be revealed by the second derivative spectra happens to the C-H groups of $[P_{4,4,4,4}][SS]$ solution upon heating. For clarity in Fig. 6(a), comparing the C-H spectrum of 20 %(w/v) $[P_{4,4,4,4}][SS]$ solution at 25 ^oC during heating with that at 25 ^oC in the cooling process, these two spectra almost overlaps with each other indicating that C-H groups can recover to the original status after a heating-cooling cycle. It is due to the revertible variation of phase transition behavior. Nevertheless, differences occur in Fig. 6(b) when it comes to the C=O groups that there are great distinctions between the absorption at 25 ^oC during heating and cooling. Besides, the integral area of C=O groups experiences decreases upon heating. Closer observation reveals an unusual phenomenon that the three spectra at 25, 41 and 50 ^oC interact at about 1628 cm^{-1}. This can be called as the isosbestic point manifesting that there is no transition state during the variation.[48, 49] In addition, we further elaborated this conclusion in the 2Dcos analysis in the following texts.

To quantitatively describe the frequencies and integral area shifting of chemical groups in the heating-cooling cycle, we plotted the detailed information in Fig. 7. According to our previous works especially on C-H groups, frequencies at about 2968, 2937, 2876 cm^{-1} can be assigned to $\nu_{as}(CH_3)$, $\nu_{as}(CH_2)$ and $\nu_s(CH_2)$ respectively.[49, 50] It can be found that both the wavenumber of $\nu_{as}(CH_3)$, $\nu_{as}(CH_2)$ and $\nu_s(CH_2)$ show obvious variations like "anti-sigmoid" shape, which are characteristic for phase transition behavior.[41]

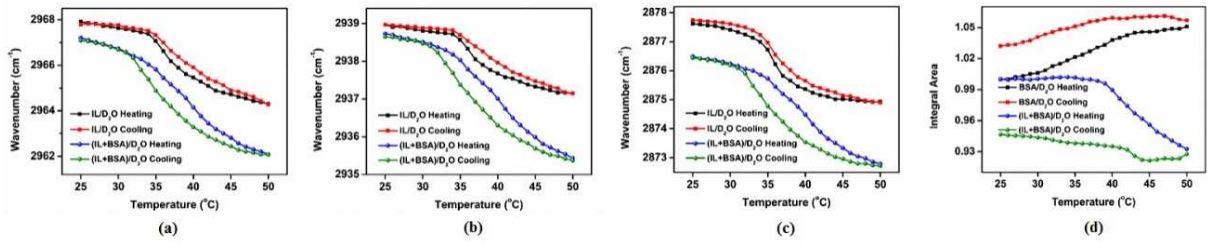

Fig. 7 Temperature-dependent frequency shifts of (a) $\nu_{as}(CH_3)$, (b) $\nu_{as}(CH_2)$, (c) $\nu_s(CH_2)$ and (d) integral area shifts of ν(C=O) in $[P_{4,4,4,4}][SS]$-BSA-D_2O solution during a heating-cooling cycle.

Although there exists a bit hysteresis phenomenon in the cooling process, the cooling curves can basically return to the original state before heating. Additionally, the hysteresis is a little bigger than the solution without BSA indicating the interactions of BSA with IL and water. However, what happens for the C=O groups is another different phenomenon. The integral area of C=O groups exhibits much different changes during the heating-cooling cycle revealing their different variations comparing with phase transition behavior. Moreover, there also appears obvious distinction between the heating and cooling curves of C=O groups that the cooling curve cannot recover to the original status before heating indicating the irrecoverable variation of C=O groups. As is mentioned in the above text, it is deduced that the variation the C=O groups upon heating is actually the irrecoverable denaturation of BSA.

Furthermore, more information can be obtained from the comparison of $[P_{4,4,4,4}][SS]$-BSA-D_2O solution with $[P_{4,4,4,4}][SS]$-D_2O or BSA-D_2O system. To come for the first, there can be found obvious distinctions in the C-H groups between the $[P_{4,4,4,4}][SS]$-BSA-D_2O tertiary system and $[P_{4,4,4,4}][SS]$-D_2O binary solution. The initial frequencies of $\nu_{as}(CH_3)$, $\nu_{as}(CH_2)$ and $\nu_s(CH_2)$ in $[P_{4,4,4,4}][SS]$-D_2O solution are a little lower than those in the mixed solution revealing the C-H groups would be a bit less hydrated with water after BSA was added. As a contrast, The three absorptions of $\nu_{as}(CH_3)$, $\nu_{as}(CH_2)$ and $\nu_s(CH_2)$ in $[P_{4,4,4,4}][SS]$-D_2O solution experienced red shifts of 3.9, 1.7 and 2.8 cm^{-1} respectively while the three peaks in $[P_{4,4,4,4}][SS]$-BSA-D_2O system underwent shifts of 5.1, 3.3 and 3.8 cm^{-1}. It means the addition of BSA into the solution makes all the frequencies of C-H groups experienced much larger shifts revealing that BSA promotes the dehydration of IL with water. It is believed by us that BSA may compete with IL to capture water molecules during the heating process which maybe attribute to the denaturation of BSA. On the other hand, the integral area of C=O groups in the $[P_{4,4,4,4}][SS]$-BSA-D_2O solution also exhibits much different changes during the heating-cooling cycle in contrast to that in the BSA-D_2O system. The integral area of C=O groups in BSA-D_2O solution exhibits a little increase which belongs to the normal variation of chemical groups without obvious changes upon heating. Its cooling process also shows some recovering tendency. However, the integral area of C=O groups with the presence of IL experienced a much different variation that it first remained unchanged and then underwent a sudden decrease upon heating which is very similar to the variation of phase transition behavior. As a contrast, the cooling curve of the C=O integral area only exhibits much weak recovery manifesting that the variation of integral area of C=O groups in the tertiary system is the combination of phase transition with denaturation. And the denaturation process is mainly initiated by the phase separation behavior.

It's known to us that the denaturation of protein is actually the transformation of different conformations in protein. To further detail these variation of different conformation in C=O groups, all the spectra of C=O stretching region were curve-fitted simultaneously over the whole temperature range. The deconvoluted spectra at 25, 39 and 50 °C are given as examples in Fig. 8(a), (b) and (c). According to the 2Dcos and second derivate results, three bands at 1670, 1650 and 1618 cm^{-1} were found. Based on previous reports,[51-55] and the experiment results, 1670, 1650 and 1618 cm^{-1} can be attributed to the absorption of α-helix and random coil, β-sheet, β-turn respectively. At the beginning of the heating process, we can know that the peak of α-helix and random coil is the main absorption while peak intensities of β-sheet and β-turn would increase with the increasing temperature. To quantitatively describe the variation of these three conformations during heating, integral areas of these three bands were depicted in Fig. 8(d), (e) and (f).

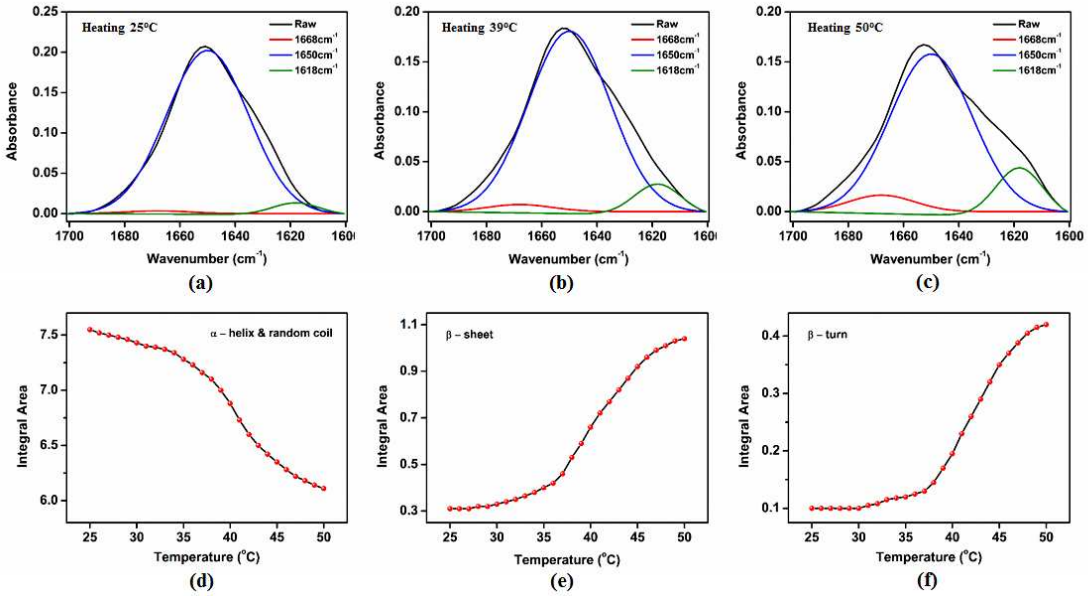

Fig. 8 Curve-fitted infrared spectra of the C=O region in $[P_{4,4,4,4}][SS]$-BSA-D_2O solution at different temperatures (a) 25 °C, (b) 39 °C, (c) 50 °C. Temperature-dependent integral area shifts of conformation of (d) α-helix and random coil, (e) β-sheet, (f) β-turn during the heating process.

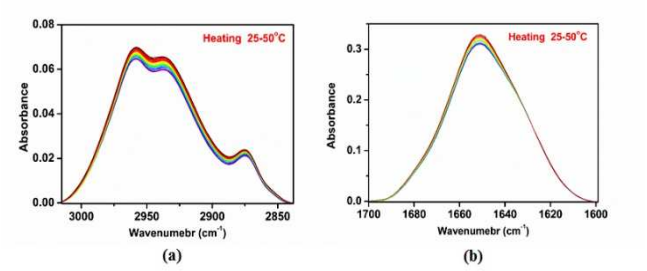

Fig. 9 Temperature-dependent FT-IR spectra of BSA-D_2O solution in the regions of (a) 3010-2840 cm^{-1}, (b) 1700-1600 cm^{-1} during heating from 25 to 50 °C.

From Fig. 8(d), the peak area of α-helix and random coil went through a slight decrease at the beginning of heating, then decreases sharply around LCST, and has a gentle change ultimately. Relatively, the integral area of β-sheet and β-turn experienced a gentle increase and then a sharp increase during the heating process, which is observed in Fig. 8(e) and (f). Combining the shifting curves of the conformation of α-helix, random coil with those of the β-sheet and β-turn conformation, it can be deduced that the variation of C=O groups is actually the transformation from α-helix and random coil to β-sheet and β-turn revealing the denaturation of BSA upon heating. This can be also supplied by the one-dimensional FTIR spectra and second derivative data. In fact, this denaturation process is initiated by the phase transition process and interactions between IL and BSA according to the variation tendency of conformations which is similar to that of phase separation behavior. Additionally, we would further demonstrate this transformation in the 2DCOS analysis in the following texts.

Now that we have analysed the variation process of phase transition of $[P_{4,4,4,4}][SS]$ and denaturation of BSA upon heating, to further confirm the interactions between $[P_{4,4,4,4}][SS]$ and BSA which may trigger the denaturation of BSA, a comparison experiment was performed. In the above measurement, ternary system which consists of $[P_{4,4,4,4}][SS]$, BSA and D_2O was prepared. There may be two reasons in this system which may induce the denaturation of BSA including the interactions of $[P_{4,4,4,4}][SS]$ with BSA and the intrinsic variation of BSA-D_2O solution. So if we can demonstrate that there are no changes in BSA-D_2O solution upon heating, then the reason for denaturation would certainly be attributed to the interactions between $[P_{4,4,4,4}][SS]$ with BSA. As a result, in the comparative experiment, only 20 wt% BSA was dissolved in D_2O which is free of IL. Due to the objective that we just want to investigate the variation tendency roughly, so the increment interval of temperature is set as 5 °C. The results of temperature-dependent FTIR spectra are illustrated in Fig. 9. Obviously, we can find that the FTIR spectra of C-H groups ranging from 3010 to 2840 cm^{-1} almost have no distinct variations during the heating process.

For further study, frequency shifts of CH and integral area shifts of C=O groups are also illustrated in Fig. 10. The frequencies of C-H groups including $\nu_{as}(CH_3)$, $\nu_{as}(CH_2)$ and $\nu_s(CH_2)$ remain nearly unchanged upon heating. Similarly, the integral area shifts of C=O groups also stay like a linear line during the heating process. It can be concluded from these data that there is no obvious change in BSA-D_2O solution during the heating process which is much different from the denaturation of BSA in the $[P_{4,4,4,4}][SS]$-BSA-D_2O ternary system. In other words, it reveals that the denaturation process of BSA was induced by interactions between $[P_{4,4,4,4}][SS]$ and BSA. In addition, the transition temperature obtained from different measurements was also presented in Fig. S1.

Perturbation correlation moving window (PCMW)

To study the details of the spectral variations and accurate phase transition temperature of different groups in $[P_{4,4,4,4}][SS]$-BSA-D_2O solution, PCMW analysis was performed. PCMW is a newly developed technique, whose basic principles can date back to conventional moving window proposed by Thomas[56], and later improved by Morita in 2006.[57] PCMW analysis provides a pair of synchronous and asynchronous two-dimensional correlation spectra between a perturbation variable (e.g., temperature) axis and a spectral variable (e.g., wavenumber) axis. Positive synchronous correlation represents the increase in spectral intensities, whereas negative correlation represents the decrement. Positive asynchronous correlation corresponds to a convex spectral intensity variation, whereas negative asynchronous correlation corresponds to a concave variation.[57] The PCMW analysis can be used to visually determine the transition points as well as the transition interval along the perturbation direction, especially weak phase transitions which are difficult to observe by other conventional methods.

Fig. 11 presents PCMW synchronous and asynchronous spectra of $[P_{4,4,4,4}][SS]$-BSA-D_2O solution during heating ranging from 25 to 50 °C. In Fig. 10, there are mainly several bands in the ν(C-H) region of 3010-2840 cm^{-1} as well as the second derivate spectra shown in Fig. 6, which include the $\nu_{as}(CH_3)$, $\nu_{as}(CH_2)$ and $\nu_s(CH_2)$ while the region of 1700-1600 cm^{-1} also has several peaks including different conformation of C=O groups. It can be

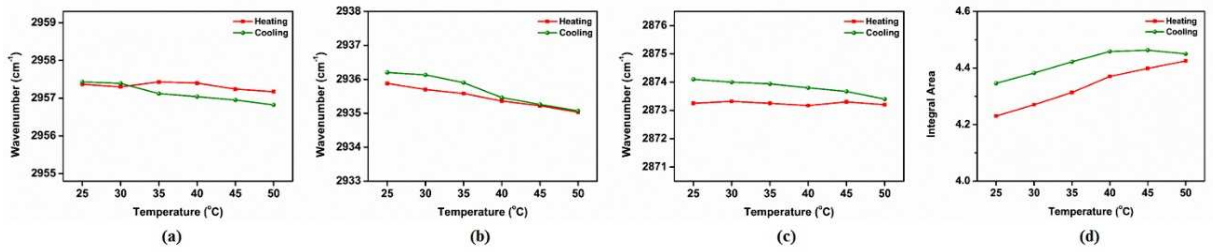

Fig. 10 Temperature-dependent frequency shifts of (a) $\nu_{as}(CH_3)$, (b) $\nu_{as}(CH_2)$, (c) $\nu_s(CH_2)$ and (d) integral area shifts of ν(C=O) in BSA-D_2O solution during a heating-cooling cycle.

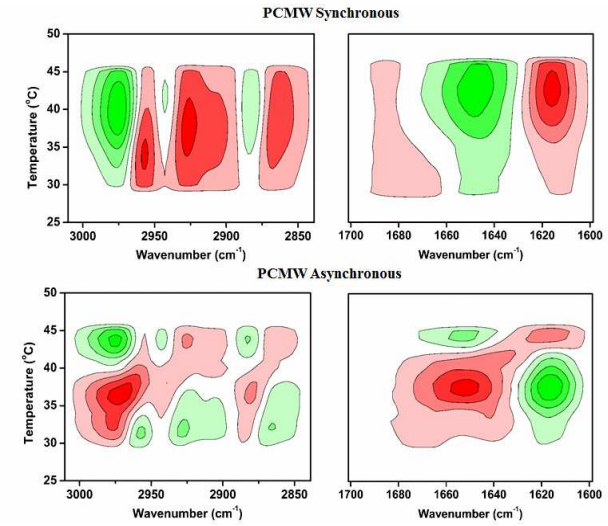

Fig. 11 PCMW synchronous and asynchronous spectra of $[P_{4,4,4,4}][SS]$-BSA-D_2O solution between 25 and 50 °C during heating. Red colors are defined as positive intensities, whereas green colors are defined as negative intensities.

detected that the transition temperature of absorption at 2958 cm^{-1} is about 34 °C, which is much lower than the transition of 2929 cm^{-1} at about 39 °C. As a contrast, the transition points of 2975, 2883 and 2865 cm^{-1} almost stay at the same temperature, 40 °C. The highest transition temperature occurs in the absorption at 2940 cm^{-1} bands which is about 41 °C. While for C=O groups, the transition temperature is little higher. The bands at 1650 cm^{-1} which belongs to the conformation of **α-**helix and random coil center at 41 °C while the transition temperature of 1670 and 1618 cm^{-1} corresponding to β-sheet and β-turn are the highest, 42 °C. Based on these data, a response order during the heating process can be obtained that (→ stands for prior to or earlier than): 2958 cm^{-1} → 2929 cm^{-1} → 2965, 2883, 2975 cm^{-1} → 1650 cm^{-1} → 2940 cm^{-1} → 1618, 1670 cm^{-1}. This sequence means that most of the C-H groups response much earlier than the C=O groups during heating, revealing the prior changes of phase transition

Table 1. Tentative band assignments of $[P_{4,4,4,4}][SS]$ and BSA according to previous reports and results of 2Dcos analysis.

Wavenumber(cm^{-1})	Assignment
2975	ν_{as}(Hydrated CH_3 in $[P_{4,4,4,4}][SS]$)
2958	ν_{as}(Dehydrated CH_3 in $[P_{4,4,4,4}][SS]$)
2940	ν_{as}(Hydrated CH_2 in $[P_{4,4,4,4}][SS]$)
2929	ν_{as}(Dehydrated CH_2 in $[P_{4,4,4,4}][SS]$)
2883	ν_{s}(Hydrated CH_2 in $[P_{4,4,4,4}][SS]$)
2865	ν_{s}(Dehydrated CH_2 in $[P_{4,4,4,4}][SS]$)
1670	β-turn conformation of BSA
1650	α-helix and random coil conformation of BSA
1618	β-sheet conformation of BSA

behavior than denaturation of BSA. For further analysis, it also indicates that the phase transition behavior behaves as the main driving force in the variation of $[P_{4,4,4,4}][SS]$ and BSA, which can be also confirmed by the following 2D correlation analysis. Furthermore, the transition temperature region can also be determined by the peaks in asynchronous spectra which are all turning points of the sigmoid curves.[42] From asynchronous spectra, we can obtain that the phase transition begins at 32 °C and comes to the end until 36 °C for the bands at 2958 cm^{-1} while the transition region of other C-H groups is mainly from 36 to 44 °C. Unlike the differences in the C-H groups, almost all the C=O groups respond simultaneously at the region ranging from 37 to 44 °C. In addition, it's worth noting that the phase separation process is able to recover to the original status before heating while the denaturation of BSA is irreversible after a cooling process, which can be demonstrated by Fig. S2 in Supporting Information.

Two-dimensional correlation spectroscopy (2DCOS)

2DCOS is a mathematical method whose basic principles were first proposed by Noda and has been used more and more widely to investigate spectral variations of chemical groups under

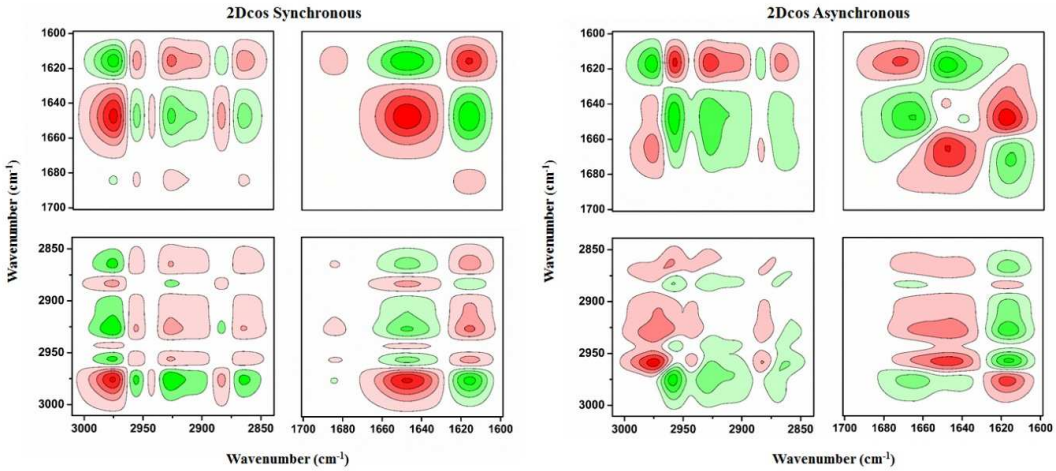

Fig. 12 2DCOS synchronous and asynchronous spectra of $[P_{4,4,4,4}][SS]$-BSA-D_2O solution during heating between 25 and 50 °C. Red colors are defined as positive intensities, while green colors as negative ones.

Table 2. The final results of multiplication on the signs of each cross-peak in synchronous and asynchronous spectra during heating.

1618	-	-	+	+	-	-	+	-	
1650	-	+	-	+	+	-	+		
1670	-	-	-	-	-	-			
2865	-	+	-	+	+				
2883	-	+	-	+					
2929	-	-	-						
2940	-	+							
2958	-								
2975									
	2975	2958	2940	2929	2883	2865	1670	1650	1618

external perturbations, such as temperature, concentration, time, pressure, and other physical variables etc.[58] It usually includes synchronous and asynchronous correlation spectra.[59] Peaks in the synchronous spectra along the diagonal are called "autopeaks", which are always positive. The off-diagonal peaks ($\Phi(\nu_1, \nu_2)$) are named as "cross-peaks", appearing in both synchronous and asynchronous spectra. The positive cross-peaks reveal that both peaks change in the same direction under the perturbation, whereas negative cross-peaks refer to changes in the opposite directions. As a result, 2DCOS synchronous spectra mainly provides information about simultaneous variations between two wavenumbers.[42] 2D asynchronous spectra can significantly enhance the spectral resolution, for instance, in Fig. 12, such as bands at 2929, 2865 cm^{-1} attributed from CH_2 groups were sorted out. These newly observed bands could significantly assist in exploring the mechanism of phase transition process. For the convenience of further discussion, all the bands detected from 2DCOS spectra and their tentative assignments have been presented in the Table 1.

Except for enhancing spectral resolution, 2DCOS can also distinguish the specific sequential order of different groups under perturbation. The sequence can be obtained according to Noda's judging rule that if the cross peaks ($\Phi(\nu_1, \nu_2)$, assume $\nu_1 > \nu_2$) in synchronous and asynchronous spectra share the same sign, the response at ν_1 occurs prior to ν_2, and vice versa.[50] Based on the analysis of PCMW, all the FT-IR spectra between 25 and 50 °C with an interval of 1 °C were applied to generate the 2DCOS spectra, as illustrated in Fig. 12.

In consideration of the relatively lengthy details of determining the sequence of spectral peaks, we chose to present the final order for heating process in Table 2. The detailed order is listed as follows (→ stands for prior to or earlier than): 2958 cm^{-1} → 2929 cm^{-1} → 2865 cm^{-1} → 2975 cm^{-1} → 2883 cm^{-1} → 1650 cm^{-1} → 1618 cm^{-1} → 2940 cm^{-1} → 1670 cm^{-1}. Or in another representation: ν_{as}(Dehydrated CH_3 in $[P_{4,4,4,4}][SS]$) → ν_{as}(Dehydrated CH_2 in $[P_{4,4,4,4}][SS]$) → ν_s(Dehydrated CH_2 in $[P_{4,4,4,4}][SS]$) → ν_{as}(Hydrated CH_3 in $[P_{4,4,4,4}][SS]$) → ν_s(Hydrated CH_2 in $[P_{4,4,4,4}][SS]$) → α-helix and random coil conformation of BSA → β-sheet conformation of BSA → ν_{as}(Hydrated CH_2 in $[P_{4,4,4,4}][SS]$) → β-turn conformation of BSA.

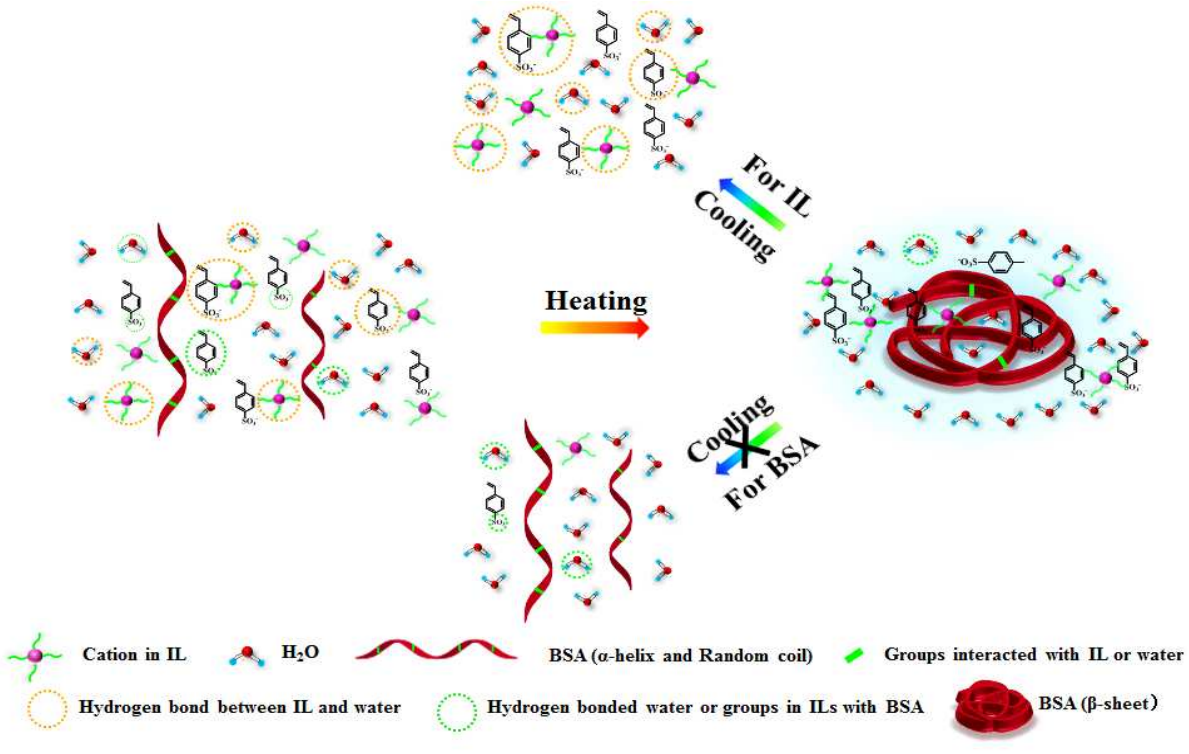

Fig. 13 Schematic illustration of the dynamic phase transition and denaturation mechanism of $[P_{4,4,4,4}][SS]$-BSA-D_2O solution during the heating and cooling process.

Without considering the differences in stretching modes, the sequence can be described as C-H groups in $[P_{4,4,4,4}][SS] \rightarrow$ α-helix and random coil conformation of BSA → β-sheet and β-turn conformation of BSA. This sequence is in good accordance with the results concluded from PCMW. For a more intuitive understanding of dynamic mechanism, the schematic illustration, Fig. 13 was presented in the text.

The sequential order indicates that the C-H groups of $[P_{4,4,4,4}][SS]$ first response to the temperature perturbation, and then the C=O groups came to respond upon heating. In fact, the response of C-H groups in IL represents the occurrence of phase separation behavior. It's the phase transition behavior of IL molecules that first take place in solution upon heating. In addition, there appears an unusual phenomenon that the dehydrated C-H of IL molecules response prior to hydrated C-H groups in the heating process. It indicates that CH groups would first experience conformational changes and then start their dehydration process in solution. Due to the interactions between $[P_{4,4,4,4}][SS]$ and BSA, phase transition behavior would initiate the denaturation of BSA through driving of these interactions between IL and BSA. That is, the $[P_{4,4,4,4}][SS]$ molecules first experience dehydration process and the hydrogen bonds between $[P_{4,4,4,4}][SS]$ and water would come to disrupt with the increase of temperature. As a result, the IL molecules would aggregate together under the driving force of hydrophobic interactions upon heating. After that, the hydrogen bonds between BSA and water or groups of IL molecules would also be disrupted upon heating. Then BSA undergoes a process of conformation changes during which the α-helix and random coil would transform to β-sheet and β-turn conformation. During the variations, the formed IL aggregated globules would distribute in a bit random manner. However, most of the water molecules would be excluded out and distribute at the periphery of the aggregates. To furthermore confirm the analysis of this dynamic process, 2DCOS spectra of the cooling process was also performed in the Supporting Information. Fig. S3 reveals that the variation of C-H groups is revertible indicating it's actually the phase transition behavior while the C=O groups of BSA after denaturation cannot recover to the original status before heating even they experienced a cooling process.

Conclusions

In this paper, DSC, turbidity, FT-IR measurements, in combination with the perturbation correlation moving window (PCMW) and two-dimensional correlation spectroscopy (2Dcos) were employed for the first time to explore the phase transition behavior of $[P_{4,4,4,4}][SS]$ and the denaturation of BSA upon heating. The molecular dynamic mechanism as well as several unusual phenomena were elucidated.

DSC results revealed the varying tendency of phase transition in $[P_{4,4,4,4}][SS]$-BSA-D_2O solutions. The transition temperature experiences a continuous increase with increasing concentration of BSA. Besides, the DSC and turbidity measurements demonstrated that the cloud point of 20 %(w/v) $[P_{4,4,4,4}][SS]$ added with 20 wt% BSA is about 39 ^oC which is 3 ^oC higher than that of 20 %(w/v) $[P_{4,4,4,4}][SS]$ indicating the existence of interactions between $[P_{4,4,4,4}][SS]$ and BSA. FTIR spectra demonstrated the hydrated interactions in solution and the dehydration process upon heating. The isosbestic point of C=O groups in the heating FTIR spectra manifests the direct transforming of BSA from α-helix, random coil to β-sheet and β-turn conformation. In other words, there is no transition state during the variation upon heating. PCMW additionally determined the different transition temperature of different chemical groups which most of the LCST of C-H groups is lower than that of C=O groups. As a contrast, the distinction between the transition region of C-H and C=O is a little small. The transition temperature regions of C-H groups are mainly from 32 to 36 ^oC and 36 to 44 ^oC while that of C=O basically ranges from 36 to 44 ^oC. Finally, 2Dcos was employed to illuminate the thermally dynamic mechanism of the changes during a heating-cooling cycle. The variations of C-H groups are mainly due to the recoverable phase transition behavior of $[P_{4,4,4,4}][SS]$ while those of the C=O groups are actually the denaturation of BSA which is irreversible. The $[P_{4,4,4,4}][SS]$ molecules tend to aggregate together under the driving of hydrophobic interactions upon heating while BSA would turn into β-sheet and β-turn conformation after heating.

Acknowledgements

We gratefully acknowledge the financial support from the National Science Foundation of China (NSFC) (Nos. **21274084)**

Notes and references

[a]*State Key Laboratory of Molecular Engineering of Polymers, Ministry of Education, Department of Macromolecular Science, and Laboratory of Advanced Materials, Fudan University, Shanghai 200433, China. E-mail: peiyiwu@fudan.edu.cn (Peiyi Wu)*

1. T. D. Ho, C. Zhang, L. W. Hantao and J. L. Anderson, *Analytical Chemistry*, 2014, **86**, 262-285.
2. X. Han and D. W. Armstrong, *Accounts of Chemical Research*, 2007, **40**, 1079-1086.
3. J. M. Lu, F. Yan and J. Texter, *Progress in Polymer Science*, 2009, **34**, 431-448.
4. A. J. Carmichael and K. R. Seddon, *Journal of Physical Organic Chemistry*, 2000, **13**, 591-595.
5. C. Chiappe and D. Pieraccini, *Journal of Physical Organic Chemistry*, 2005, **18**, 275-297.
6. J. Mo, L. J. Xu and J. L. Xiao, *Journal of the American Chemical Society*, 2005, **127**, 751-760.
7. V. I. Parvulescu and C. Hardacre, *Chemical Reviews*, 2007, **107**, 2615-2665.
8. F. van Rantwijk and R. A. Sheldon, *Chemical Reviews*, 2007, **107**, 2757-2785.
9. G. A. Baker, S. N. Baker, S. Pandey and F. V. Bright, *Analyst*, 2005, **130**, 800-808.
10. M. Armand, F. Endres, D. R. MacFarlane, H. Ohno and B. Scrosati, *Nature Materials*, 2009, **8**, 621-629.
11. H. T. Liu, Y. Liu and J. H. Li, *Physical Chemistry Chemical Physics*, 2010, **12**, 1685-1697.
12. D. Mecerreyes, *Progress in Polymer Science*, 2011, **36**, 1629-1648.

13. J. Y. Yuan, D. Mecerreyes and M. Antonietti, *Progress in Polymer Science*, 2013, **38**, 1009-1036.
14. R. M. Vrikkis, K. J. Fraser, K. Fujita, D. R. MacFarlane and G. D. Elliott, *Journal of Biomechanical Engineering-Transactions of the Asme*, 2009, **131**.
15. H. Ohno and Y. Fukaya, *Chemistry Letters*, 2009, **38**, 2-7.
16. J. A. Laszlo and D. L. Compton, *Journal of Molecular Catalysis B-Enzymatic*, 2002, **18**, 109-120.
17. S. N. Baker, T. M. McCleskey, S. Pandey and G. A. Baker, *Chemical Communications*, 2004, 940-941.
18. K. Fujita, D. R. MacFarlane and M. Forsyth, *Chemical Communications*, 2005, 4804-4806.
19. Z. Du, Y. L. Yu and J. H. Wang, *Chemistry-a European Journal*, 2007, **13**, 2130-2137.
20. Y. C. Pei, J. J. Wang, K. Wu, X. P. Xuan and X. J. Lu, *Separation and Purification Technology*, 2009, **64**, 288-295.
21. X. Q. Ding, Y. Z. Wang, Q. Zeng, J. Chen, Y. H. Huang and K. J. Xu, *Analytica Chimica Acta*, 2014, **815**, 22-32.
22. T. Li, B. L. Li, S. J. Dong and E. K. Wang, *Chemistry-a European Journal*, 2007, **13**, 8516-8521.
23. M. L. Pusey, M. S. Paley, M. B. Turner and R. D. Rogers, *Crystal Growth & Design*, 2007, **7**, 787-793.
24. D. Hekmat, D. Hebel, S. Joswig, M. Schmidt and D. Weuster-Botz, *Biotechnology Letters*, 2007, **29**, 1703-1711.
25. E. Y. Chi, S. Krishnan, T. W. Randolph and J. F. Carpenter, *Pharmaceutical Research*, 2003, **20**, 1325-1336.
26. D. Constantinescu, H. Weingartner and C. Herrmann, *Angewandte Chemie-International Edition*, 2007, **46**, 8887-8889.
27. D. Constatinescu, C. Herrmann and H. Weingartner, *Physical Chemistry Chemical Physics*, 2010, **12**, 1756-1763.
28. A. M. Figueiredo, J. Sardinha, G. R. Moore and E. J. Cabrita, *Physical Chemistry Chemical Physics*, 2013, **15**, 19632-19643.
29. S. Soll, M. Antonietti and J. Y. Yuan, *Acs Macro Letters*, 2012, **1**, 84-87.
30. Y. B. Xiong, J. J. Liu, Y. J. Wang, H. Wang and R. M. Wang, *Angewandte Chemie-International Edition*, 2012, **51**, 9114-9118.
31. Y. Kohno, H. Arai, S. Saita and H. Ohno, *Australian Journal of Chemistry*, 2011, **64**, 1560-1567.
32. P. Nockemann, K. Binnemans, B. Thijs, T. N. Parac-Vogt, K. Merz, A. V. Mudring, P. C. Menon, R. N. Rajesh, G. Cordoyiannis, J. Thoen, J. Leys and C. Glorieux, *Journal of Physical Chemistry B*, 2009, **113**, 1429-1437.
33. H. Yoshimitsu, A. Kanazawa, S. Kanaoka and S. Aoshima, *Macromolecules*, 2012, **45**, 9427-9434.
34. K. Fukumoto and H. Ohno, *Angewandte Chemie-International Edition*, 2007, **46**, 1852-1855.
35. Y. J. Men, H. Schlaad and J. Y. Yuan, *Acs Macro Letters*, 2013, **2**, 456-459.
36. Y. Kohno and H. Ohno, *Chemical Communications*, 2012, **48**, 7119-7130.
37. Y. Kohno and H. Ohno, *Physical Chemistry Chemical Physics*, 2012, **14**, 5063-5070.
38. Y. Maeda, in *Polymer-Solvent Complexes and Intercalates - Polysolvat 8*, ed. J. M. Guenet, 2011, vol. 303.
39. W. T. Li and P. Y. Wu, *Polymer Chemistry*, 2014, **5**, 761-770.
40. Y. Kohno and H. Ohno, *Australian Journal of Chemistry*, 2012, **65**, 91-94.
41. S. T. Sun and P. Y. Wu, *Macromolecules*, 2013, **46**, 236-246.
42. W. L. Li and P. Y. Wu, *Soft Matter*, 2013, **9**, 11585-11597.
43. S. T. Sun and P. Y. Wu, *Journal of Physical Chemistry B*, 2011, **115**, 11609-11618.
44. P. M. Reddy and P. Venkatesu, *Journal of Physical Chemistry B*, 2011, **115**, 4752-4757.
45. Y. Maeda, T. Nakamura and I. Ikeda, *Macromolecules*, 2002, **35**, 217-222.
46. H. N. Lee and T. P. Lodge, *Journal of Physical Chemistry Letters*, 2010, **1**, 1962-1966.
47. H. N. Lee, N. Newell, Z. F. Bai and T. P. Lodge, *Macromolecules*, 2012, **45**, 3627-3633.
48. B. Sun, Y. Lin, P. Wu and H. W. Siesler, *Macromolecules*, 2008, **41**, 1512-1520.
49. H. N. Wang, S. T. Sun and P. Y. Wu, *Journal of Physical Chemistry B*, 2011, **115**, 8832-8844.
50. S. T. Sun, P. Y. Wu, W. D. Zhang, W. Zhang and X. L. Zhu, *Soft Matter*, 2013, **9**, 1807-1816.
51. C. E. Giacomelli, M. Bremer and W. Norde, *Journal of Colloid and Interface Science*, 1999, **220**, 13-23.
52. V. Militello, C. Casarino, A. Emanuele, A. Giostra, F. Pullara and M. Leone, *Biophysical Chemistry*, 2004, **107**, 175-187.
53. P. Bourassa, C. D. Kanakis, P. Tarantilis, M. G. Pollissiou and H. A. Tajmir-Riahi, *Journal of Physical Chemistry B*, 2010, **114**, 3348-3354.
54. P. Bourassa, I. Hasni and H. A. Tajmir-Riahi, *Food Chemistry*, 2011, **129**, 1148-1155.
55. D. H. Tsai, F. W. DelRio, A. M. Keene, K. M. Tyner, R. I. MacCuspie, T. J. Cho, M. R. Zachariah and V. A. Hackley, *Langmuir*, 2011, **27**, 2464-2477.
56. M. Thomas and H. H. Richardson, *Vibrational Spectroscopy*, 2000, **24**, 137-146.
57. S. Morita, H. Shinzawa, I. Noda and Y. Ozaki, *Applied Spectroscopy*, 2006, **60**, 398-406.
58. I. Noda, *Journal of Molecular Structure*, 2008, **883**, 2-26.
59. I. Noda, *Journal of the American Chemical Society*, 1989, **111**, 8116-8118.

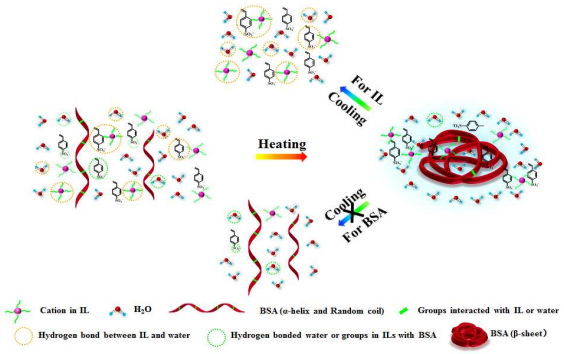

dynamic phase transition and denaturation mechanism of $[P_{4,4,4,4}][SS]$-BSA-D_2O solution during the heating and cooling process.